Going in the right direction

Cellular mechanisms underlying root halotropism

Korver, R.A.

Publication date
2019

Document Version
Other version

License
Other

Chapter 6

Epsin-like clathrin adaptors, ECA1 and ECA4 control halotropism in distinct ways without affecting PIN2 localization

Ruud A. Korver[1], Simone Lambregts[1], Jessica Meyer[1,2] & Christa Testerink[1,2]

[1]Plant Cell Biology, Swammerdam Institute for Life Sciences, University of Amsterdam, The Netherlands
[2]Plant Physiology, Department Plantenwetenschappen, Wageningen University & Research, The Netherlands

Abstract

Clathrin-mediated endocytosis has been linked to auxin-carrier cycling in unstressed cells. Nevertheless, the endocytosis pathway involved in salt stress remains elusive. Recently, two Epsin-like clathrin adaptors (ECA1 and ECA4) were found enriched in the peripheral membrane fraction of salt-stressed Arabidopsis roots. Here, we investigate a possible role of ECA1 and ECA4 in the halotropic response, root system architecture and subcellular localization of the auxin-efflux carrier, Pin-formed 2 (PIN2) during salt stress. Additionally, we screened for proteins that interact with ECA4 using a tandem-affinity purification assay. Proteins identified were involved in cell division, vacuolar sorting and actin cytoskeleton organization. During halotropism, opposite phenotypes were found for ECA1- and ECA4- KO mutants. Loss-of-ECA4 also resulted in longer main and lateral roots and a higher lateral root density. Using a GFP fusion, ECA1 was found to be enriched in the cytosol upon salt treatment. However, following PIN2-GFP in an *eca1* and *eca4* background revealed no changes in the sub-cellular localization of PIN2 compared to wildtype. Our results indicate roles for ECA1 and ECA4 during salt stress, in cellular processes that are not linked to PIN2 localization.

Introduction

The recent increase of farmland affected by abiotic stress has put more pressure on the development of tolerant crops to maintain food production. Fortunately, advancements in technology have helped to speed-up the selection of tolerant mutants during forward genetic screening, but often, the reason for increased tolerances is not known. Understanding underlying cellular mechanisms of abiotic stress tolerance helps us to comprehend what processes are most important during different types of stress encountered in the environment. In this way, even more viable, tolerant lines with no pleiotropic effects might be selected or engineered. One process involved in all cellular changes caused by abiotic stress, and most processes in general, is cellular signalling. To start a signalling cascade, stress first needs to be sensed.

For salinity stress, and the sensing of the toxic ion, Na^+, the signalling mechanism is still largly unknown, despite some theories proposed (see (Maathuis, 2014; Julkowska and Testerink, 2015; Shabala et al., 2015). Nonetheless, some early signalling components have been characterized. The calcium dependent-SOS pathway has been well described (Ji et al., 2013). Another early salt-induced signal is the lipid second messenger phosphatidic acid (PA) (Munnik, 2001; Testerink and Munnik, 2005, 2011). In contrast to

structural lipids, signalling lipids are found in low abundance in cellular membrane. However, upon sensing of stress, their abundance can increase within minutes (Munnik et al., 2000; Darwish et al., 2009; Meringer et al., 2016). The stress-induced formation of PA has been proposed to be phospholipase D (PLD) and/or phospholipase C (PLC)/diacylglycerol kinase (DGK) dependent (Munnik et al., 2000; Munnik, 2001; Darwish et al., 2009; Arisz and Munnik, 2011; Meringer et al., 2016). The difference in involvement of the PLD and the PLC/DGK pathways might be in the timing, where PLC/DGK act on a short-term time scale (Munnik et al., 2000; van der Luit et al., 2000; de Jong et al., 2004; Arisz et al., 2013), and PLD is involved in PA production on a time scale of hours (Frank et al., 2000; Munnik et al., 2000; Ruelland et al., 2002; Arisz et al., 2003; Andersson et al., 2006; Hong et al., 2009; Hong et al., 2010). Cytosolic target proteins have been found to bind PA (Testerink et al., 2004; McLoughlin et al., 2013). Such proteins are thought to be recruited to the PM or other intracellular membrane compartments where PA accumulates. PA-binding proteins in plants include Heat Shock Protein 90 (HSP90), 14-3-3 proteins, ROOTS CURL IN NPA (RCN1) and SNF1-RELATED PROTEIN KINASE 2.10 (SnRK2.10) (Testerink et al., 2004), which all play a role on abiotic stress responses (Roberts et al., 2002; Baena-Gonzalez and Sheen, 2008; Xu et al., 2012; Hu et al., 2017; Yao and Xue, 2018). Downstream of lipid signalling during salt stress, several hormone signalling pathways are known, for example salicylic acid (Jayakannan et al., 2015) and gibberellins (Colebrook et al., 2014). How these signalling pathways are linked, however, remains elusive. Using PA-affinity purification on proteins isolated from the peripheral membrane fraction after salt stress, eight PA-binding proteins were found, including three proteins involved in the clathrin machinery: Clathrin Heavy Chain (CHC), Epsin-like Clathrin Adaptor 1 (ECA1) and Epsin-like Clathrin Adaptor 4 (ECA4) (McLoughlin et al., 2013). Interestingly, clathrin-mediated endocytosis has been proposed to be involved in the internalization and recycling of auxin carriers (Kleine-Vehn et al., 2011; Adamowski and Friml, 2015; Naramoto, 2017). Recently, ECA1 and ECA4 were found to locate to the growing cell plate during cell division (Song et al., 2012). Due to the role for AP180 N-terminal homology (ANTH)/Epsin N-terminal homology (ENTH) domain-containing proteins in clathrin coated vesicle (CCV) formation (Legendre-Guillemin et al., 2004); ECA1 and ECA4 were proposed to regulate CCV budding from the cell plate. In support, ECA4 was found to interact with TPLATE complex muniscin-like (TML), which forms multi protein-complexes with, amongst others, the TPLATE protein complex and CHC and CLC,

confirming the involvement of ECA4 in CME (Gadeyne et al., 2014). Other than this, nothing is known about ECA1 and ECA4 in plant processes.

During salt stress, CME was proposed to alter the flow of auxin in the root and subsequently, the direction of root growth (Galvan-Ampudia et al., 2013). Recently, it was shown that NAA pre-treatment (which blocks clathrin recruitment to the PM), did not block the accumulation of Pin-formed 2 (PIN2) inside cells during salt stress (Baral et al., 2015). Depletion of sterols, however, did inhibit its intracellular accumulation, suggesting the possible involvement of membrane microdomain-associated endocytosis (MMAE) in the internalization of PIN2 during salt stress (Baral et al., 2015). Likewise, PIN1 has been found in detergent-resistant membrane (DRM) fractions (sterol-rich domains, also known as membrane microdomains) when treated with Triton X-100 in wild type plants. In *abcb19* mutants, this occurred much less, indicating that PIN1 could be present in membrane-microdomains where it is stabilized by ABCB19 (Titapiwatanakun et al., 2009). While the question remains which endocytic pathway(s) regulate the internalization of auxin carriers during salt stress, ECA1 and ECA4's lipid-binding enrichment in response to salt in the peripheral membrane protein fraction, and their link to CME, warrants investigation of their role in salt stress.

Here, we analysed ECA1 and ECA4 single- and double-KO mutants during halotropism and investigated their root system architecture (RSA) upon salt stress. Using an ECA1-GFP fusion, the effect of salt stress on its localization was analysed, as well as its co-localization with CLC2. For PIN2, its dynamics as GFP fusion during salt stress in wildtype and *eca1*- and *eca4* seedlings were analysed. Our results suggest that while ECA1 and ECA4 are involved in the plants' response to salt stress, they are neither involved in PIN2 internalization nor polarity. Using tandem-affinity purification, several proteins were found to interact with ECA4, i.e. proteins involved in cell division, vacuolar sorting and energy flux.

Results

ECA1 and ECA4 have opposite roles during halotropism

We used a time-lapse set-up to study early halotropic responses in an *eca1*-, *eca4*- and *eca1/eca4*- double mutant and compared that with wild type. Only minor differences were observed between any of the *eca* mutants and wildtype in the first 12 hrs after exposing them to the salt gradient (Supplemental figure 1). However, after 13 hrs, significant differences with wildtype were found in the *eca4* and *eca1/eca4* mutants (Supplemental figure 1). Where the double-

knockout mutant did not bend and followed the gravital axis, *eca4* was found to bend at an angle of -10° away from the salt gradient. The halotropic response has a duration of various days and the initial response at the first day has only a minor contribution to the total avoidance. So in addition to the early response, we also measured the directional root growth over 4 days on plates containing a gradient of 0mM, 75mM, 125mM or 200 mM of NaCl (Figure 1a-d). No differences in root growth direction between the *eca* mutants and wildtype were observed in control conditions (Figure 1a). Nonetheless, in contrast to the early response, large differences in root growth direction were observed in *eca* mutants during long-term exposure to a 125mM or 200mM salt gradient (Figure 1c-d). Clearly, *eca1* showed a weaker halotropic response than wild type while *eca4* showed a significant stronger response than wild type on a 200mM NaCl salt gradient (Figure 1d). The response in the *eca1/eca4*-double mutant showed maybe the net effect of the two individual mutants, resembling wild type (Figure 1d).

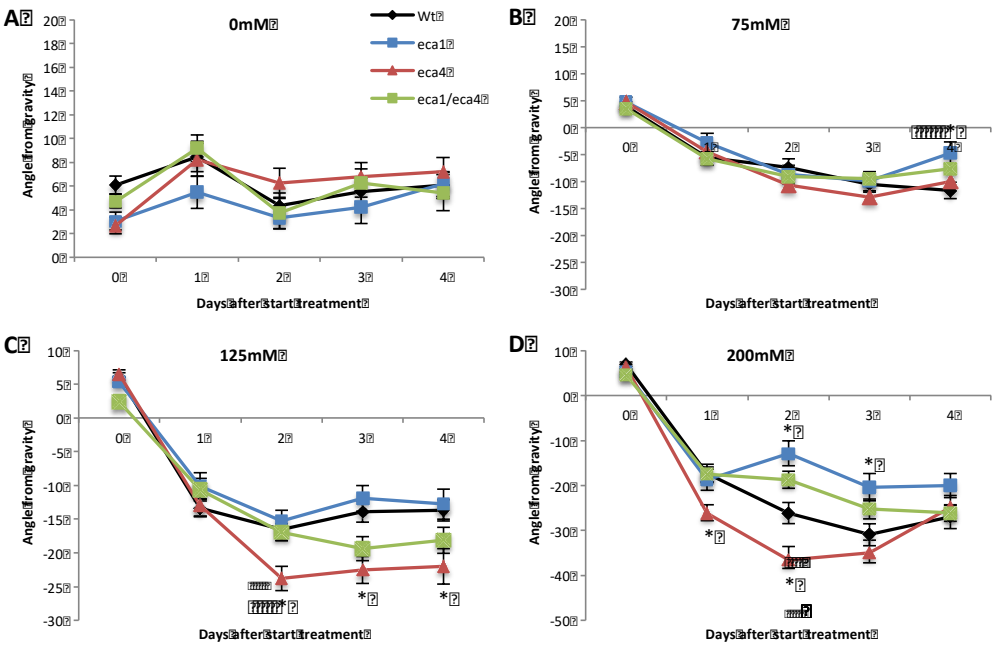

Figure 1: Late halotropic responses of the *eca1*, *eca4* and *eca1/eca4* KO mutants show opposite phenotypes for ECA1 and ECA4 during halotropism. Root tip angle during late halotropic response in the *eca1*, *eca4* and *eca1/eca4* KO mutants compared to wildtype on 0mM (A), 75mM (B), 125mM (C) or 200mM (D) NaCl. Bars represent standard error. Asterisks show significant differences with wildtype ($p<0.05$, univariate ANOVA followed by Tukey's post hoc test in SPSS 24). Data shown is combined from 2 biological replicates N > 40 for each line and treatment.

Loss-of-ECA4 promotes root growth and -development

Proteins involved in the internalization of auxin carriers not only regulate tropism responses, they also affect the root system architecture (Bao et al., 2014; Li et al., 2015; Korver et al., Chapter 4 this thesis). Hence, we tested the role of ECA1 and ECA4 in RSA during control and salt stress using the KO mutants. As shown in Figure 2a, the main roots of *eca4* seedlings were longer in control- and salt stress conditions (Figure 2a). Moreover, *eca4* mutants also exhibited more and longer lateral roots (figure 2b-c), resulting in a higher total root- and lateral root length (Supplemental figure 2a-b). While none of these differences were induced by salt treatment, lateral root density in *eca4* was clearly higher than wildtype on 75mM- and 125mM NaCl, but not without salt (Figure 2d-e). The *eca4* roots were also found to be less straight, and exhibited a longer branched zone (Supplemental figure 2c-d). For *eca1*, no such differences were observed, nor in the *eca1/eca4*-double mutant (Figure 2 and Supplemental figure 2).

ECA1-GFP is internalized upon salt stress and co-localizes with clathrin-light chain

To further understand ECA1's role in halotropism, we determined the subcellular localization of ECA1-GFP under its own promoter (Song et al., 2012). Under control conditions, ECA1 was mainly localized to the PM, with a low signal in the cytosol, as described before (Song et al., 2012). Within 5 min after salt treatment, the PM signal decreased and the cytosolic signal of ECA1-GFP clearly increased in the epidermal roots cells at the lower part of the elongation zone (Figure 3a-b). This increased cytosolic ECA1 localization remained visible for at least 60 min. To determine whether the internalization of ECA1 was linked to CME, the co-localization between ECA1-GFP and CLC2-mCherry was investigated. As shown in Figure 3c-d, a significant increase in ECA1 and CLC co-localization occurred upon salt stress. These results indicate increased association of ECA1 with CME during salt stress.

ECA1 and ECA4 do not affect the internalization of PIN2 during salt stress

The increased co-localization of ECA1 and CLC in the cytosol 5 min after the application of salt may suggest an increase in CME, and hence, the increased internalization of auxin carriers upon salt stress. To investigate a putative involvement of ECA1 in the alteration of auxin flow during salt stress, we studied the sub-cellular localization of PIN2-GFP in in the *eca1* and *eca4* mutant backgrounds. Interestingly, no change in PIN2 localization was observed after 5 or 60 min of salt stress in either mutant (Figure 4). These results suggest that

the internalization or polarity of PIN2 during early salt stress responses of roots is independent ECA1 or ECA4.

ECA4 interacts with proteins putatively involved in cell division, vacuolar sorting, cell polarity and energy flux

To further analyse the cellular processes ECA1 and ECA4 might be involved in, tandem-affinity purification (TAP) analyses in PSB-D Arabidopsis suspension-cultured cells were performed to identify direct- and indirect ECA interactors (Puig et al., 2001; Gadeyne et al., 2014). Unfortunately, TAP analysis using ECA1 as bait protein did not reveal any interacting proteins. Using ECA4, however, 13 possible interactors were found after filtering-out known contaminants (Table 1, Supplemental Table S1). Amongst these were both Clathrin Heavy Chain (CHC) isoforms and both clathrin light chain (CLC) proteins identified, even though the latter was not found in all experiments and in lower

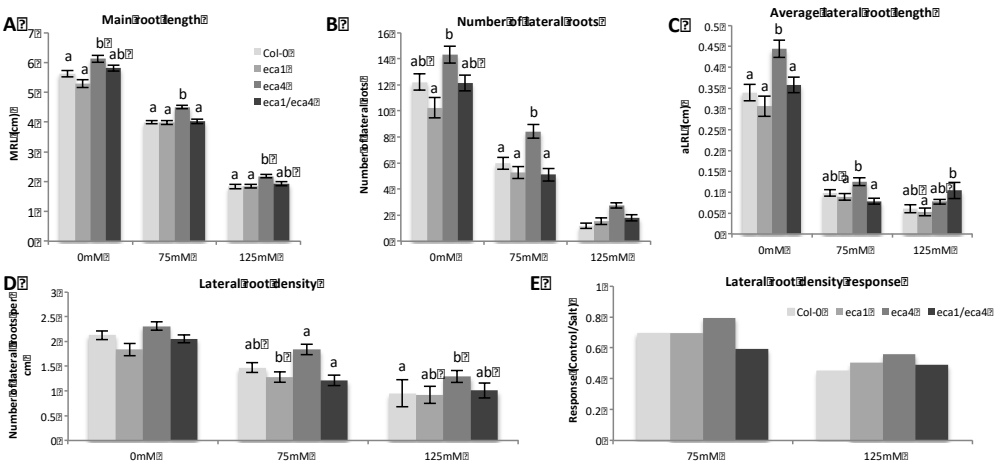

Figure 2: *eca4* has altered RSA and a salt specific higher lateral root density. 10 day old Arabidopsis seedlings were scanned after growth on plates with different salt concentrations (0mM, 75mM and 125mM NaCl). Different root parameters were analyzed using Smartroot. Seedlings were transferred to the treatment plates four days after germination, and treated for 6 days. Significant differences for *eca4* were found for main root length (A), number of lateral roots (B), average lateral root length (C) and lateral root density (D). Lateral root density had only significant differences in salt treatment therefore response to salt was plotted (E). Error bars represent standard error and letters show different significance groups, no letters means no differences ($p<0.05$, in a univariate ANOVA followed by Tukey's post hoc test in SPSS 24). N = 40 roots from 2 biological replicates.

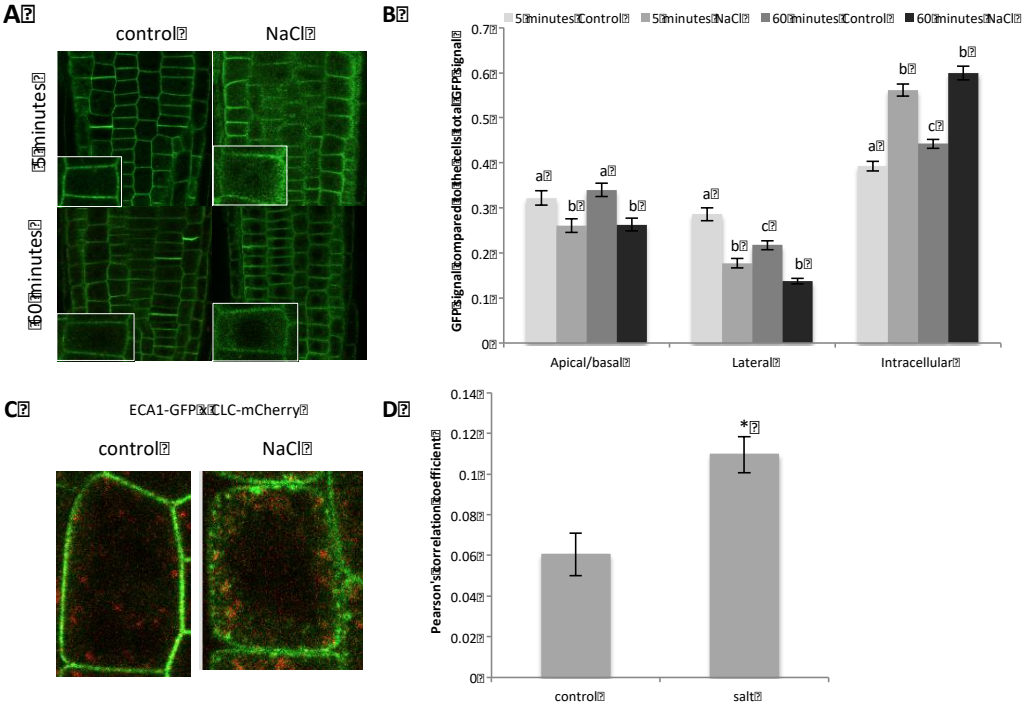

Figure 3: ECA1 re-locates to the cytosol during salt stress and has increased co-localization with CLC. (A) Representative images showing ECA1-GFP after 5 and 60 minutes during a control and a salt treatment. (B) Quantification of ECA1-GFP signal intensity on the apical membrane, the lateral membrane and the intracellular compartment compared to the total GFP signal in the cell. Letters show different significance groups per PM side between the different treatments ($p<0.05$, in a univariate ANOVA followed by Tukey's post hoc test in SPSS 24) ($n > 56$ cells per treatment over 2 biological replicates). (C) Representative images of ECA1-GFP (green) and CLC-mCherry (red) after 5 minutes of a control or salt treatment, yellow color shows co-localization. (D) Quantification of ECA1-GFP and CLC-mCherry co-localization using Pearson's Correlation Coefficient (PCC). Perfect co-localized images score 1 on this scale while images without any co-localization score -1. Asterisks show significance ($p<0.05$, in a t-test performed with SPSS 24) (N = 20 cells per treatment from 2 biological replicates).

abundance. Other proteins found in all 4 experiments (with both C-terminal and N-terminal tagged ECA4) were COP1-interactive protein 1 (CIP1, AT5G41790) and voltage dependent anion channel 1 (VDAC1, AT3G01280) (Table 1). Putative interactors found in 3 experiments, included a P-loop containing nucleoside triphosphate hydrolases superfamily protein (At3G45850) and an Endosomal targeting BRO1-like domain-containing protein (At1G15130). Proteins only found in one or two experiments, suggesting indirect binding or false positives, were Clathrin Associated Protein 1 (CAP1) (At4G32285), little nuclei1 (LINC1) (Dittmer et al., 2007), PRP39 (At1G04080) (Wang et al., 2007) and a RNA-binding (RRM/RBD/RNP motifs) family protein (At2G33410).

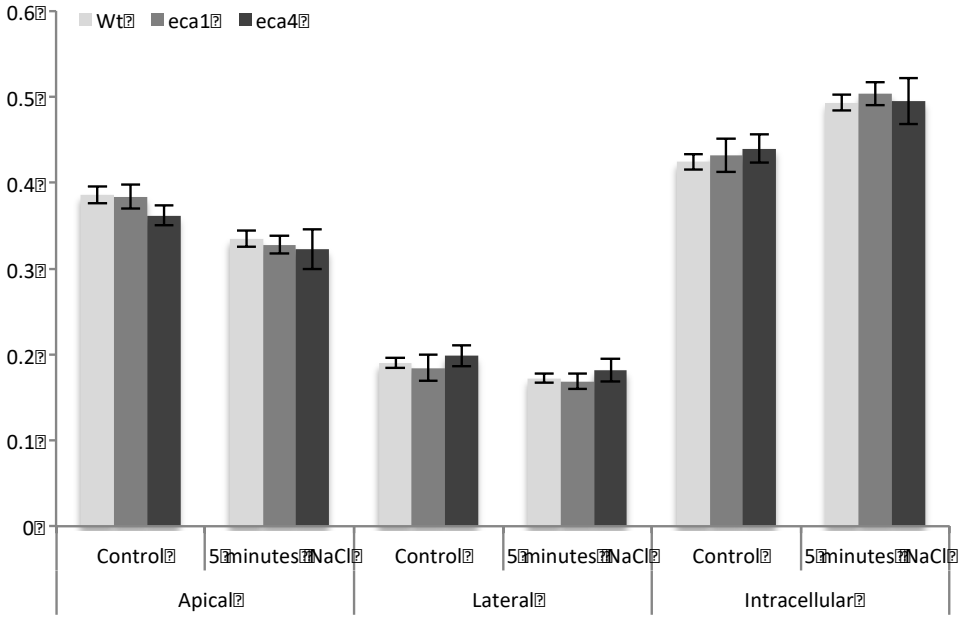

Figure 4: No change of PIN2 sub-cellular localization in *eca1* and *eca4* mutants. *eca1* and *eca4* have the same PIN2 polarity and salt-induced polarity shift after 5 minutes compared to wildtype. No differences in abundance of PIN-GFP signal was observed at either apical, lateral or the intracellular compartment during control or salt treatment. ($p<0.05$, in an univariate ANOVA followed by Tukey's post hoc test in SPSS 24). For Wt, n=80 cells, for *eca1*, n=48 cells, for *eca4*, n= 48 cells in 2 biological replicates.

Table 1: ECA4 TAP-tag interactors. Four experiments were conducted, twice with a N-terminal tag and twice with a C-terminal tag. Asterisks show interactions found in the different experiments. Thirteen interactions remained after filtering-out known contaminants. Functions of proteins without reference are based on computational methods by arabidopsis.org.

At number	N-terminal tag experiment 1	N-terminal tag experiment 2	C-terminal tag experiment 1	C-terminal tag experiment 2	Score	Protein description	Literature
AT3G11130	*	*	*	*	4	Clathrin, heavy chain	
AT3G08530	*	*	*	*	4	Clathrin, heavy chain	
AT2G25430	*	*	*	*	4	epsin N-terminal homology (ENTH) domain-containing protein / clathrin assembly protein-related	Song *et al.*, 2012
AT5G41790	*	*	*	*	4	CIP1 | COP1-interactive protein 1	Ren et al., 2016
AT3G01280	*	*	*	*	4	VDAC1, ATVDAC1 | voltage dependent anion channel 1	Pan et al., 2014 ; Robert et al., 2012 ; Lee et al., 2009
AT3G45850		*	*	*	3	P-loop containing nucleoside triphosphate hydrolases superfamily protein	Not available
AT5G67500	*	*	*		3	VDAC2, ATVDAC2 | voltage dependent anion channel 2	Robert et al., 2012; Lee et al., 2009 ; Yan et al., 2009
AT1G15130	*	*	*		3	Endosomal targeting BRO1-like domain-containing protein	Not available
AT4G32285	*	*			2	ENTH/ANTH/VHS superfamily protein	Song *et al.*, 2012
AT2G20760	*	*			2	Clathrin light chain protein	
AT1G67230		*			1	LINC1 | little nuclei1	Dittmer *et al.*, 2007
AT2G40060	*				1	Clathrin light chain protein	
AT1G04080				*	1	PRP39 | Tetratricopeptide repeat (TPR)-like superfamily protein	Wang *et al.*, 2007
AT2G33410				*	1	RNA-binding (RRM/RBD/RNP motifs) family protein	

We searched the STRING database for interactions of At3G45850 and At1G15130 to elucidate their function (Table 2). At3G45850 was, amongst others, predicted to interact with Mitotic Arrest Deficient 2 (MAD2), Structural Maintenance of Chromosomes 2 (SMC2), Structural Maintenance of Chromosomes 3 (SMC3) and At2G20635, which have all been predicted to play a role during the cell cycle, specifically checkpoints during nuclear division. Predicted interactions with At1G15130 include SNF family proteins SNF7.2 and SNF7.1. Both these proteins are a component of the endosomal-sorting complex required for transport III (ESCRT-III) complex which is involved in vacuolar protein sorting (Cai et al., 2014). Additionally, At1G15130 was predicted to interact with RAC-like 2 (RAC2), RAC-like 3 (RAC3 or ROP6), RAC-like 6 (RAC6), ARAC-like 9 (RAC9) and Rho-related protein from plants 1 (ROP1), which all belong to the family of small GTPases involved in signalling, in particular in regulation of the cytoskeleton. Although the interactions remain to be confirmed, these interacting proteins imply a role for ECA4 in various membrane transport processes.

Discussion

In this study, we investigated the role of ECA1 and ECA4 during salt stress, including the halotropic response and root system architecture. In addition, the subcellular localization of ECA1 in combination with CLC was determined, as well as the localization of PIN2. Finally, putative protein-protein interactions were performed to find new leads for the processes in which ECAs play a role during salt stress.

ECA1 and ECA4 are involved in the late halotropic response

Loss-of-ECA1 or -ECA4 only had no clear effect on the early halotropic response (first 24 hrs) but affected the later response, 2-4 days after exposure. Interestingly, *eca1* seedlings showed a weaker response while *eca4* seedlings lead to a stronger halotropic response. This clearly indicates distinct roles for these clathrin adaptors during halotropism. Unlikely, this difference is explained by the involvement of PIN2 because we found no changes in its localization in the loss-of-function mutants. A possible explanation might be found in the observation that ECA1 plays a more important role in cell plate formation during cytokinesis (Song et al., 2012), and thus loss-of-ECA1 could potentially inhibit initiation of cytokinesis, although it remains unclear whether renewed cell division is required for halotropism.

According to the eFP browser (Winter et al., 2007), ECA4 expression is elevated at the lower part of the root-elongation zone, in contrast to the constitutive overall expression of ECA1, which may imply a role in cell elongation. The possible indirect interaction with Rac-like G-proteins in the TAP assay could support such a role. The involvement of the different ECAs in different processes might lead to the observed differences in the halotropic response. However, much remains unclear about the function of the ECA's and the processes they are involved in, so this requires more research.

Table 2: Predicted interactions of At3G45850 and At1G15130 show respectively putative involvement in mitosis and cell polarity. Interactions were predicted by the STRING database and are based on co-expression.

Protein	At number	Interactor	Description
P-loop containing nucleoside triphosphate hydrolases superfamily protein	AT3G45850	AT2G20635	catalytic domain of protein kinase and Mad3-BUB1-I domain-containing protein
		AT3G54630	Kinetochore protein NDC80
		AT5G05510	Mad3/BUB1 homology region 1
		PPK1	Putative protein kinase 1
		MAD2	MITOTIC ARREST-DEFICIENT 2; Required for the execution of the mitotic checkpoint which monitors the process of kinetochore-spindle attachment
		EMB2656	EMBRYO DEFECTIVE 2656
		AT4G15890	
		ATSMC2	Member of SMC subfamily; Central component of the condensin complex
		SMC2	SMC2-1 (SMC2); Central component of the condensin complex
		SMC3	Member of SMC subfamily; Central component of the condensin complex
Endosomal targeting BRO1-like domain-containing protein	AT1G15130	SNF7.2	vacuolar protein sorting-associated protein 32-1; Component of the ESCRT-III complex
		SNF7.1	vacuolar protein sorting-associated protein 32-2; Component of the ESCRT-III complex
		SKD1	SUPPRESSOR OF K+ TRANSPORT GROWTH DEFECT1; Involved in the transport of biosynthetic membrane proteins from the prevacuolar/endosomal compartment to the vacuole.
		AT1G08270	Uncharacterized protein
		UPL5	Ubiquitin protein ligase 5, regulation of leaf senescence
		RAC2	RAC-like 2; Inactive GDP-bound Rho GTPases reside in the cytosol
		RAC6	RAC-like 6; putatively involved in cell polarity control during the actin-dependent tip growth of pollen tubes
		RAC3	RAC-like 3; Inactive GDP-bound Rho GTPases reside in the cytosol. SPK1-dependent activation is required for auxin-mediated inhibition of PIN2 internalization during gravitropic responses (Lin *et al.*, 2012)
		ROP1	RHO-related protein from plants 1; May be involved in cell polarity control during the actin-dependent tip growth of pollen tubes. May regulate callose synthase 1 (CALS1) activity through the interaction with UGT1
		ARAC9	Arabidopsis RAC-like 9; Inactive GDP-bound Rho GTPases reside in the cytosol

ECA4 negatively regulates root size and lateral root formation

A change in the halotropic response, as found in loss-of-ECA1 and -ECA4 mutants, suggests changes of auxin flow in the root. Such changes also influence root development, including lateral root initiation (De Smet, 2012; Marhavy et al., 2013). Adjusting the number- and length of lateral roots is another important part of the plant's response to salt stress (Zolla et al., 2010; Julkowska et al., 2014). Here, we found increased main root length, number of lateral roots and lateral root length in the ECA4 loss-of-function mutant under both control and salt stress conditions. Moreover, lateral root density in the *eca4* mutant showed a salt-specific increase, indicating a role for ECA4 in alterations in RSA during the salt stress response. The *eca1* mutant behaved similar as wildtype on

both control and salt stress conditions. These results emphasize that ECA1 and ECA4 fulfil distinct roles in roots, with ECA4 but not ECA1 playing a role in lateral root formation. Support for this theory comes from transcriptomic analysis of Arabidopsis roots in response to auxin, where ECA4 was found to have reduced pericycle expression after auxin treatment while ECA1 expression did not change (Bargmann et al., 2013). In contrast to ECA1, which putatively is involved in initiation of cytokinesis, ECA4 could possibly inhibit the asymmetric cell division at the pericycle, which is required for lateral root initiation through its role at the cell plate. This is consistent with ECA4 being more abundant at the forming cell plate while ECA1 is mostly found later, at the edges of the expanding cell plate (Song et al., 2012). Moreover, it has been shown that CME is involved in the plane of cell division through syntaxin localization (Boutte et al., 2010). If ECA4 is involved in inhibiting the CME-dependent process regulating cell-plate position and thus asymmetric cell division, loss-of-ECA4 might explain an increased number of lateral roots and density. However, the exact role of ECA4 in lateral root formation and root length requires more attention before a definitive answer can be given.

PIN2 localization is not regulated by ECA1 or ECA4

We found ECA1 re-localization from the plasma membrane to the intracellular compartment shortly after exposure to salt and this increased cytosol localization remained unchanged after an hour of salt stress. This re-localization coincides with an increase in colocalization with CLC-mCherry. These results confirm the biochemical experiments by McLoughlin *et al.* (2013) and indicate a salt induced ECA1 mediated CME during the salt stress response. Nevertheless, a recent study using NAA, a known inhibitor of CME, found PIN2 internalization despite blocking CME, indicating clathrin-independent endocytosis during salt stress (Baral et al., 2015). On the other hand, CME has been proposed to be involved in PIN2 internalization during halotropism (Galvan-Ampudia et al., 2013). Thus, it remains unclear whether ECA1 might regulate auxin carrier internalization. However, because the shift in PIN2 polarity was not found after 60 min (unpublished data) and the ECA1 increase in the cytosol was unaltered after 60 min, it seems unlikely the ECA1 mediates the CME involved in this process. In accordance, we see no change in PIN2 localization in either control or salt stress in *eca1*- or *eca4* mutants compared to wild type.

ECA4 interacts with proteins involved in cell division, vacuolar sorting and the actin cytoskeleton

Both ECA1 and ECA4 were used as bait for tandem-affinity purification, however, only ECA4-interacting proteins were found. Amongst the interactors found were COP-interactive protein 1 (CIP1) and Arabidopsis Voltage Dependent Anion Channel 1 and 2 (VDAC1 and VDAC2). CIP1 is induced by abscisic acid (ABA) in photosynthetic and vascular tissue. VDAC1 and VDAC2 locate mainly to the outer-mitochondrial membrane and in low abundance to the PM (Robert et al., 2012). No change in VDAC1 and VDAC2 transcript levels was found during salinity stress (Lee et al., 2009). No evidence for involvement of CIP1 or both VDAC's in stressed roots has been reported, therefore we focused on other interactors. Two other strong interacting proteins found, i.e. P-loop containing nucleoside triphosphate hydrolases superfamily protein (PNTH) and Endosomal targeting BRO1-like domain-containing protein (EtB), have not been characterized, and their function is only predicted. Documented interactions in the STRING database can provide information on the processes involved. For PNTH, interactions with proteins involved in cell cycle regulation were predicted, based on interactions in *Saccharomyces cerevisiae* (MAD2, SMC2, SMC3 and At2G20635) (Tong et al., 2004). Arrest of the cell cycle during salt stress has been reported (West et al., 2004) and might play a role during the quiescence phase of root growth during salt stress, or potentially during halotropism, in addition to inhibition of cell elongation. In order to determine the role in cell-cycle regulation during salt stress further research is needed. Using cell-cycle markers (Yin et al., 2014), the percentage of cells in different phases could be examined on both sides of the root during the halotropic response, for example. EtB was predicted to interact with components of the Endosomal Sorting Complex Required for Transport III (ESCRT-III), SNF7.1 and SNF7.2, and thus could be involved in protein sorting to the vacuole (Cai et al., 2014). Moreover, EtB was predicted to interact with Suppressor of K^+ Transport Growth Defect1 (SKD1), which has also been reported to be involved in vacuolar sorting (Herberth et al., 2012; Steffens et al., 2017). Although we did not observe a PIN2 subcellular-localization phenotype nor difference in abundance, ECA4 might play a role in vacuolar targeting and thus degradation of PIN2 and other auxin carriers during long-term salt exposure of roots. Other interactors of EtB include RAC-like 2, 3, 6 (RAC2, RAC3, RAC6) and Arabidopsis RAC-like 9 (ARAC9). RAC3 has been shown to be involved in the auxin-induced re-orientation of the actin cytoskeleton organization (Chen et al., 2014). In this way, ECA4 could potentially be a negative regulator of cell elongation according to the indirect interaction with RAC3 and the stronger halotropic response of

the *eca4* KO mutant. To further elucidate the role of ECA4, the actin cytoskeleton could be studied in the *eca4* mutant. Overall, the TAP experiment lead to two interesting new genes, At3G45850 and At1G15130, which are potentially involved in the salt stress response in the root. Overall, we show promising interactions of ECA4 with At3G45850 and At1G15130 supporting a role for ECA4 in salt-induced processes involved in cell division, vacuolar sorting and actin cytoskeleton organization.

Methods

Tandem affinity purification

TAP-tag was performed using protein G and Streptavidin-binding peptide (GS)-tagged bait ECA1 and ECA4 protein fusions on all proteins from Arabidopsis cell culture cells (PSB-D) according to (Van Leene et al., 2011).

Plant material and growth conditions

The wild type used was *Arabidopsis thaliana* ecotype Columbia-0 (Col-0). The *eca1* mutant is a tDNA insertion line (Salk_114631). The *eca4* mutant is a tDNA insertion line from GABI-KAT (GABI_839F07). The *eca1/eca4* double mutant was created by crossing both single mutants. Knockouts were confirmed by qPCR. Genotyping primers used, ECA1 forward gtagatcacagaaatcaacgc, ECA1 reverse ggttcaacaactcgcctc, ECA4 forward taaagttcttacggcaaaagcaga and ECA4 reverse ttgcttgctactttagcg. Primers used for qPCR, ECA1 forward ctgatttctatgaagcctgc, ECA1 reverse gaagctatgtaggctccatc, ECA4 forward aggatttcgaatttcgttaggttcg and ECA4 reverse tcgccgaatctcacaacgc. The ECA1-GFP x CLC-mCherry line was obtained from Inwhan Hwang (Song et al., 2012). The PIN2-GFP x *eca1* line was created by crossing the *eca1* and PIN2-GFP (kindly received from Remko Ofringa, Leiden University).

General growth conditions on agar plates (half strength MS supplemented with 0.1% 2(N-morpholino)ethanesulphonic acid (MES) buffer and 0.5% Sucrose and 1% Agar) were in a climate chamber with long day period (16 hrs light at 130 μmol/m^2/s) at 22°C and 70% humidity. Seeds were sterilized using 50% bleach and stratified for at least 2 days at 4°C. For soil experiments, seeds sterilized with 50% bleach were stratified in 0,1% agar in the dark for at least 2 days and then placed on sieved sowing ground. Plants were then grown were in a climate chamber with short day period (11 hrs light at 130 μmol/m^2/s) at 22°C and 70% humidity.

Halotropism plate assays and gravitropism plate assays

For the halotropism plate assays (both during timelapse imaging and long-term halotropism assays) 10 seeds were germinated in a diagonal line on half strength MS plates. When the seedlings were 5 days old, the bottom corner (in diagonal line 0.5 cm below the root tips) of the agar was removed and replaced by control half strength MS agar without salt or half strength MS agar containing 200 mM NaCl. For the time-lapse

experiment the plates were placed in a climate chamber containing the time-lapse set-up. Here, all plates were imaged every 20 min by infrared photography. Images were then analysed using ImagJ. For the long-term halotropism assay a dot was placed immediately after replacing the agar and every 24 hrs after the start of the treatment. After 4 days of growth, plates were scanned and the images analysed using ImageJ.

Root system architecture assay:
eca1, *eca4, eca1/eca4* and WT plants were germinated on half strength MS plates. Four days after germination the seedlings were transferred to half strength MS plates with either 0 mM, 75 mM and 125 mM of NaCl. Four seedlings were transferred to each plate, resulting in 20 replicas per line per treatment. Plates were placed in the climate chamber following a randomized order. After 6 days the plates were scanned using an Epson Perfection V800 scanner at a resolution of 400 dpi. Root phenotypes were quantified using the SmartRoot (Lobet et al., 2011) plugin for ImageJ. Statistical analysis was performed in R with RStudio using two-way ANOVA with Tukey's post-hoc test for significance.

Confocal microscopy
The images were acquired using a Nikon Ti inverted microscope in combination with an A1 spectral confocal scanning head. For GFP fusion proteins excitation/emission wavelengths used were 488 nm/505-555 nm. For mCherry the excitation/emission wavelengths were 561 nm/570-620 nm. The analysis of the images was performed using Fiji (http://fiji.sc) software. All measured membranes were corrected for their size so the artificial unit used depicts average transport capacity over the membrane.

Salt performance assay:
eca1, *eca4, eca1/eca4* and WT plants were germinated on sowing soil. After one week of growth seedlings were transferred to the treatment trays in a randomized order, with 2 seedlings per pot. A day before transfer of seedlings the dried treatment trays were treated with 4L of rainwater containing entonem salt for a final concentration of 75 mM NaCl or no salt for the control treatment. Per line per treatment 20 replicates are used. After one week of growth on the treatment tray the seedlings were thinned to one seedling per pot, when necessary seedlings from the same tray and genotype were transferred to an empty pot. The trays were watered with rainwater once per week. Three weeks after the start of the treatment the shoots the plants were

Acknowledgements
We would like to thank Inhwan Hwang (Pohang University of Science and Technology, South Korea) for the ECA1-GFP line and advice on ECA KO mutants. We would like to acknowledge Nancy De Winne (the cloning, cultures and the TAP experiment), Geert De Jaeger & Eugenia Russinova (Department of Plant Biotechnology and Bioinformatics, Ghent University, 9052 Ghent, Belgium and

Center for Plant Systems Biology, VIB, 9052 Ghent, Belgium) for the TAP experiment. Additionally, we thank Michel Haring and Teun Munnik for critical reading and advice. This project was funded by NWO (CW 711.014.002).

References

Adamowski M, Friml J (2015) PIN-dependent auxin transport: action, regulation, and evolution. Plant Cell **27:** 20-32

Andersson MX, Kourtchenko O, Dangl JL, Mackey D, Ellerstrom M (2006) Phospholipase-dependent signalling during the AvrRpm1- and AvrRpt2-induced disease resistance responses in Arabidopsis thaliana. Plant J **47:** 947-959

Arisz SA, Munnik T (2011) The salt stress-induced LPA response in Chlamydomonas is produced via PLA(2) hydrolysis of DGK-generated phosphatidic acid. J Lipid Res **52:** 2012-2020

Arisz SA, Valianpour F, van Gennip AH, Munnik T (2003) Substrate preference of stress-activated phospholipase D in Chlamydomonas and its contribution to PA formation. The Plant J **24:** 595-604

Arisz SA, van Wijk R, Roels W, Zhu JK, Haring MA, Munnik T (2013) Rapid phosphatidic acid accumulation in response to low temperature stress in Arabidopsis is generated through diacylglycerol kinase. Front Plant Sci **4:** 1

Baena-Gonzalez E, Sheen J (2008) Convergent energy and stress signaling. Trends Plant Sci **13:** 474-482

Bao Y, Aggarwal P, Robbins NE, 2nd, Sturrock CJ, Thompson MC, Tan HQ, Tham C, Duan L, Rodriguez PL, Vernoux T, Mooney SJ, Bennett MJ, Dinneny JR (2014) Plant roots use a patterning mechanism to position lateral root branches toward available water. Proc Natl Acad Sci U S A **111:** 9319-9324

Baral A, Irani NG, Fujimoto M, Nakano A, Mayor S, Mathew MK (2015) Salt-Induced Remodeling of Spatially Restricted Clathrin-Independent Endocytic Pathways in Arabidopsis Root. Plant Cell**:** tpc-15

Bargmann BO, Vanneste S, Krouk G, Nawy T, Efroni I, Shani E, Choe G, Friml J, Bergmann DC, Estelle M, Birnbaum KD (2013) A map of cell type-specific auxin responses. Mol Syst Biol **9:** 688

Boutte Y, Frescatada-Rosa M, Men S, Chow CM, Ebine K, Gustavsson A, Johansson L, Ueda T, Moore I, Jurgens G, Grebe M (2010) Endocytosis restricts Arabidopsis KNOLLE syntaxin to the cell division plane during late cytokinesis. EMBO J **29:** 546-558

Cai Y, Zhuang X, Gao C, Wang X, Jiang L (2014) The Arabidopsis Endosomal Sorting Complex Required for Transport III Regulates Internal Vesicle Formation of the Prevacuolar Compartment and Is Required for Plant Development. Plant Physiol **165:** 1328-1343

Chen X, Grandont L, Li H, Hauschild R, Paque S, Abuzeineh A, Rakusova H, Benkova E, Perrot-Rechenmann C, Friml J (2014) Inhibition of cell expansion by rapid ABP1-mediated auxin effect on microtubules. Nature **516:** 90-93

Colebrook EH, Thomas SG, Phillips AL, Hedden P (2014) The role of gibberellin signalling in plant responses to abiotic stress. J Exp Biol **217:** 67-75

Darwish E, Testerink C, Khalil M, El-Shihy O, Munnik T (2009) Phospholipid signaling responses in salt-stressed rice leaves. Plant Cell Physiol **50:** 986-997
de Jong CF, Laxalt AM, Bargmann BO, de Wit PJ, Joosten MH, Munnik T (2004) Phosphatidic acid accumulation is an early response in the Cf-4/Avr4 interaction. Plant J **39:** 1-12
De Smet I (2012) Lateral root initiation: one step at a time. New Phytologist **193:** 867-873
Dittmer TA, Stacey NJ, Sugimoto-Shirasu K, Richards EJ (2007) LITTLE NUCLEI genes affecting nuclear morphology in Arabidopsis thaliana. Plant Cell **19:** 2793-2803
Frank W, Munnik T, Kerkmann K, Salamani F, Bartels D (2000) Water Deficit Triggers Phospholipase D Activity in the Resurrection Plant Craterostigma plantagineum. Plant Cell **12:** 111-123
Gadeyne A, Sanchez-Rodriguez C, Vanneste S, Di Rubbo S, Zauber H, Vanneste K, Van Leene J, De Winne N, Eeckhout D, Persiau G, Van De Slijke E, Cannoot B, Vercruysse L, Mayers JR, Adamowski M, Kania U, Ehrlich M, Schweighofer A, Ketelaar T, Maere S, Bednarek SY, Friml J, Gevaert K, Witters E, Russinova E, Persson S, De Jaeger G, Van Damme D (2014) The TPLATE adaptor complex drives clathrin-mediated endocytosis in plants. Cell **156:** 691-704
Galvan-Ampudia CS, Julkowska MM, Darwish E, Gandullo J, Korver RA, Brunoud G, Haring MA, Munnik T, Vernoux T, Testerink C (2013) Halotropism is a response of plant roots to avoid a saline environment. Curr Biol **23:** 2044-2050
Herberth S, Shahriari M, Bruderek M, Hessner F, Muller B, Hulskamp M, Schellmann S (2012) Artificial ubiquitylation is sufficient for sorting of a plasma membrane ATPase to the vacuolar lumen of Arabidopsis cells. Planta **236:** 63-77
Hong Y, Devaiah SP, Bahn SC, Thamasandra BN, Li M, Welti R, Wang X (2009) Phospholipase D epsilon and phosphatidic acid enhance Arabidopsis nitrogen signaling and growth. Plant J **58:** 376-387
Hong Y, Zhang W, Wang X (2010) Phospholipase D and phosphatidic acid signalling in plant response to drought and salinity. Plant Cell Environ **33:** 627-635
Hu R, Zhu Y, Wei J, Chen J, Shi H, Shen G, Zhang H (2017) Overexpression of PP2A-C5 that encodes the catalytic subunit 5 of protein phosphatase 2A in Arabidopsis confers better root and shoot development under salt conditions. Plant Cell Environ **40:** 150-164
Jayakannan M, Bose J, Babourina O, Shabala S, Massart A, Poschenrieder C, Rengel Z (2015) The NPR1-dependent salicylic acid signalling pathway is pivotal for enhanced salt and oxidative stress tolerance in Arabidopsis. J Exp Bot **66:** 1865-1875
Ji H, Pardo JM, Batelli G, Van Oosten MJ, Bressan RA, Li X (2013) The Salt Overly Sensitive (SOS) pathway: established and emerging roles. Mol Plant **6:** 275-286
Julkowska MM, Hoefsloot HC, Mol S, Feron R, de Boer GJ, Haring MA, Testerink C (2014) Capturing Arabidopsis root architecture dynamics with ROOT-FIT reveals diversity in responses to salinity. Plant Physiol **166:** 1387-1402
Julkowska MM, Testerink C (2015) Tuning plant signaling and growth to survive salt. Trends Plant Sci **20:** 586-594

Kleine-Vehn J, Wabnik K, Martiniere A, Langowski L, Willig K, Naramoto S, Leitner J, Tanaka H, Jakobs S, Robert S, Luschnig C, Govaerts W, Hell SW, Runions J, Friml J (2011) Recycling, clustering, and endocytosis jointly maintain PIN auxin carrier polarity at the plasma membrane. Mol Syst Biol **7:** 540

Legendre-Guillemin V, Wasiak S, Hussain NK, Angers A, McPherson PS (2004) ENTH/ANTH proteins and clathrin-mediated membrane budding. J Cell Sci **117:** 9-18

Li G, Song H, Li B, Kronzucker HJ, Shi W (2015) Auxin Resistant1 and PIN-FORMED2 Protect Lateral Root Formation in Arabidopsis under Iron Stress. Plant Physiol **169:** 2608-2623

Lobet G, Pages L, Draye X (2011) A novel image-analysis toolbox enabling quantitative analysis of root system architecture. Plant Physiol **157:** 29-39

Maathuis FJ (2014) Sodium in plants: perception, signalling, and regulation of sodium fluxes. J Exp Bot **65:** 849-858

Marhavy P, Vanstraelen M, De Rybel B, Zhaojun D, Bennett MJ, Beeckman T, Benkova E (2013) Auxin reflux between the endodermis and pericycle promotes lateral root initiation. EMBO J **32:** 149-158

McLoughlin F, Arisz SA, Dekker HL, Kramer G, de Koster CG, Haring MA, Munnik T, Testerink C (2013) Identification of novel candidate phosphatidic acid-binding proteins involved in the salt-stress response of Arabidopsis thaliana roots. Biochem J **450:** 573-581

Meringer MV, Villasuso AL, Margutti MP, Usorach J, Pasquaré SJ, Giusto NM, Machado EE, Racagni GE (2016) Saline and osmotic stresses stimulate PLD/diacylglycerol kinase activities and increase the level of phosphatidic acid and proline in barley roots. Environ Exp Bot **128:** 69-78

Munnik T (2001) Phosphatidic acid: an emerging plant lipid second messenger. Trends Plant Sci **6:** 227-233

Munnik T, Meijer HJG, ter Riet B, Hirt H, Wolfgang F, Bartels D, Musgrave A (2000) Hyperosmotic stress stimulates phospholipase D activity and elevates the levels of phosphatidic acid and diacylglycerol pyrophosphate. Plant J **22:** 147-154

Naramoto S (2017) Polar transport in plants mediated by membrane transporters: focus on mechanisms of polar auxin transport. Curr Opin Plant Biol **40:** 8-14

Puig O, Caspary F, Rigaut G, Rutz B, Bouveret E, Bragado-Nilsson E, Wilm M, Seraphin B (2001) The tandem affinity purification (TAP) method: a general procedure of protein complex purification. Methods **24:** 218-229

Roberts RR, Salinas J, Collinge DB (2002) 14-3-3 proteins and the response to abiotic and biotic stress. Plant Mol Biol **50:** 1031-1039

Ruelland E, Cantrel C, Gawer M, Kader JC, Zachowski A (2002) Activation of phospholipases C and D is an early response to a cold exposure in Arabidopsis suspension cells. Plant Physiol **130:** 999-1007

Shabala S, Wu H, Bose J (2015) Salt stress sensing and early signalling events in plant roots: Current knowledge and hypothesis. Plant Sci **241:** 109-119

Song K, Jang M, Kim SY, Lee G, Lee GJ, Kim DH, Lee Y, Cho W, Hwang I (2012) An A/ENTH domain-containing protein functions as an adaptor for clathrin-coated vesicles on the growing cell plate in Arabidopsis root cells. Plant Physiol **159:** 1013-1025

Steffens A, Jakoby M, Hulskamp M (2017) Physical, Functional and Genetic Interactions between the BEACH Domain Protein SPIRRIG and LIP5 and SKD1 and Its Role in Endosomal Trafficking to the Vacuole in Arabidopsis. Front Plant Sci **8:** 1969

Testerink C, Dekker HL, Lim ZY, Johns MK, Holmes AB, Koster CG, Ktistakis NT, Munnik T (2004) Isolation and identification of phosphatidic acid targets from plants. Plant J **39:** 527-536

Testerink C, Munnik T (2005) Phosphatidic acid: a multifunctional stress signaling lipid in plants. Trends Plant Sci **10:** 368-375

Testerink C, Munnik T (2011) Molecular, cellular, and physiological responses to phosphatidic acid formation in plants. J Exp Bot **62:** 2349-2361

Tong AHY, Lesage G, Bader GD, Ding H, Xu H, Xin X, Young J, Berriz GF, Brost RL, Chang M (2004) Global mapping of the yeast genetic interaction network. science **303:** 808-813

van der Luit AH, Piatti T, van Doorn A, Musgrave A, Felix G, Boller T, Munnik T (2000) Elicitation of Suspension-Cultured Tomato Cells Triggers the Formation of Phosphatidic Acid and Diacylglycerol Pyrophosphate. Plant Physiol **123:** 1507-1515

Van Leene J, Eeckhout D, Persiau G, Van De Slijke E, Geerinck J, Van Isterdael G, Witters E, De Jaeger G (2011) Isolation of transcription factor complexes from Arabidopsis cell suspension cultures by tandem affinity purification. Methods Mol Biol **754:** 195-218

Wang C, Tian Q, Hou Z, Mucha M, Aukerman M, Olsen OA (2007) The Arabidopsis thaliana AT PRP39-1 gene, encoding a tetratricopeptide repeat protein with similarity to the yeast pre-mRNA processing protein PRP39, affects flowering time. Plant Cell Rep **26:** 1357-1366

West G, Inze D, Beemster GT (2004) Cell cycle modulation in the response of the primary root of Arabidopsis to salt stress. Plant Physiol **135:** 1050-1058

Winter D, Vinegar B, Nahal H, Ammar R, Wilson GV, Provart NJ (2007) An "Electronic Fluorescent Pictograph" browser for exploring and analyzing large-scale biological data sets. PLoS One **2:** e718

Xu ZS, Li ZY, Chen Y, Chen M, Li LC, Ma YZ (2012) Heat shock protein 90 in plants: molecular mechanisms and roles in stress responses. Int J Mol Sci **13:** 15706-15723

Yao HY, Xue HW (2018) Phosphatidic acid plays key roles regulating plant development and stress responses. J Integr Plant Biol

Yin K, Ueda M, Takagi H, Kajihara T, Sugamata Aki S, Nobusawa T, Umeda-Hara C, Umeda M (2014) A dual-color marker system for in vivo visualization of cell cycle progression in Arabidopsis. Plant J **80:** 541-552

Zolla G, Heimer YM, Barak S (2010) Mild salinity stimulates a stress-induced morphogenic response in Arabidopsis thaliana roots. J Exp Bot **61:** 211-224

Supplemental information

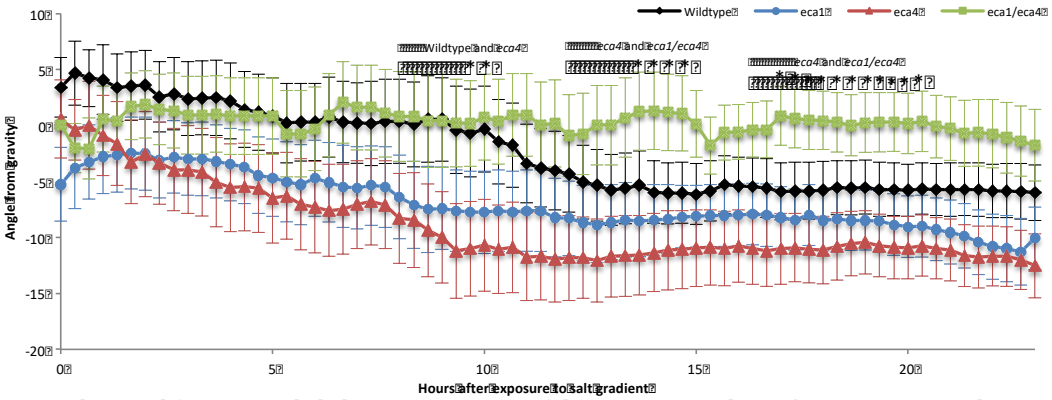

Supplemental figure 1: Early halotropic responses of the *eca1, eca4* and *eca1/eca4* KO mutants show minor differences between mutants and wildtype. Time-lapse results for the early halotropic response. Root tip angle was calculated for every 20 minutes after application of the salt gradient where growth straight down corresponds with 0 degrees and growth away from the higher salt gradient corresponds with negative angles. Bars represent standard error, asterisks show significant differences ($p<0.05$, in a univariate ANOVA followed by Tukey's post hoc test in SPSS 24). N = ±40 for all lines, data is combined from 2 biological replicates.

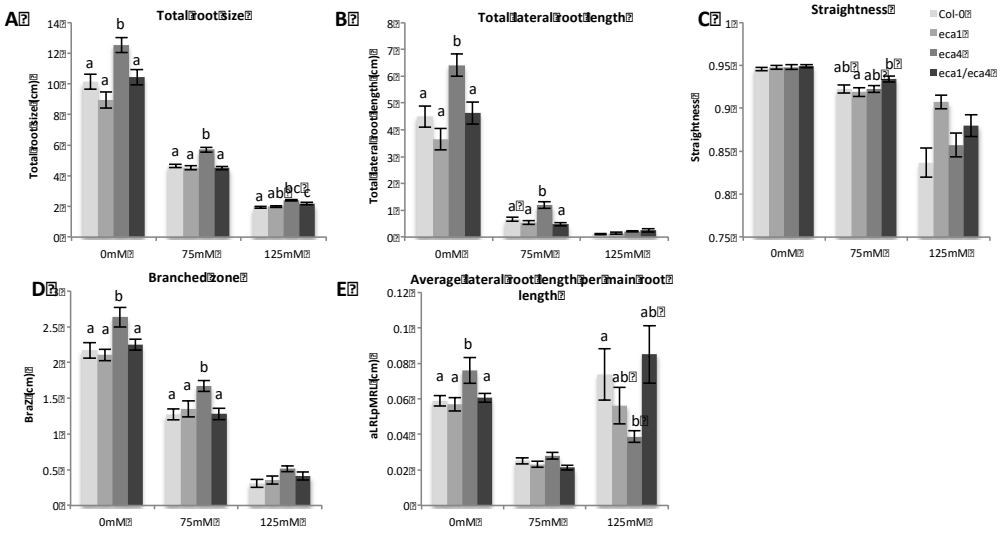

Supplemental figure 2: *eca4* has minor changes in RSA on control and salt stress. 10 day old Arabidopsis seedlings were scanned after growth on plates with different salt concentrations (0mM, 75mM and 125mM). Different root parameters were analyzed using Smartroot. Seedlings were transferred to the treatment plates four days after germination, and treated for 6 days. Significant differences for *eca1/eca4* were found for straightness (A). For *eca4* for total root size (B), total lateral root length (C), branched zone (D) and average lateral root per main root length (E). Error bars represent standard error and letters show different significance groups, no letters means no differences ($p<0.05$, in a univariate ANOVA followed by Tukey's post hoc test in SPSS 24). N = 40 roots from 2 biological replicates.

Supplemental table 1: All proteins found during TAP-tag with ECA4 as bait.

AT-number	protein description	protein score	protein mass	significant protein matches	significant protein sequences	protein coverage	protein length
AT3G11130	Clathrin, heavy chain	2914	194433	83	68	45.6	1705
AT3G08530	Clathrin, heavy chain	2813	194402	83	66	43.2	1703
AT2G25430	epsin N-terminal homology (ENTH) domain-containing protein / clathrin assembly protein-related	2066	72267	61	30	54.2	653
AT5G41790	CIP1 | COP1-interactive protein 1	378	182038	12	12	9.2	1586
AT3G01280	VDAC1, ATVDAC1 | voltage dependent anion channel 1	321	29464	10	10	42.8	276
AT3G45850	P-loop containing nucleoside triphosphate hydrolases superfamily protein	156	119734	5	5	5.8	1058
AT5G67500	VDAC2, ATVDAC2 | voltage dependent anion channel 2	103	29634	4	4	14.5	276
AT1G15130	Endosomal targeting BRO1-like domain-containing protein	134	95605	4	4	6.9	846
AT4G32285	ENTH/ANTH/VHS superfamily protein	624	70795	22	14	26.6	635
AT2G20760	Clathrin light chain protein	160	37202	5	4	8.6	338
AT1G67230	LINC1 | little nuclei1	139	129471	5	5	5.4	1132
AT2G40060	Clathrin light chain protein	76	28876	3	3	8.1	258
AT1G04080	PRP39 | Tetratricopeptide repeat (TPR)-like superfamily protein	55	85417	3	3	4.3	768
AT2G33410	RNA-binding (RRM/RBD/RNP motifs) family protein	65	41303	2	2	5.7	404